

C. Thomas Foxon\*

## Molecular beam epitaxy

Au cours des dix dernières années, une nouvelle méthode utilisant une technologie ultra-vide a été développée pour la préparation des composés binaires et pseudo-binaires III-V. Cette technique connue maintenant sous le nom d'építaxie par jets moléculaires (MBE : *Molecular Beam Epitaxy*) est une version très améliorée de l'évaporation sous vide. Elle permet de faire croître des couches minces tout en contrôlant précisément la composition chimique, la perfection cristalline et les niveaux de dopage. On atteint cette précision en alimentant l'interface de croissance en quantités contrôlées de matière, à partir de sources à jets moléculaires. On discute dans cet article de la technologie nécessaire, de l'état des connaissances sur les processus qui contrôlent la croissance, la composition et l'incorporation de dopant. On étudie les propriétés du GaAs homoépítaxial et des films multicouches de GaAs-Ga<sub>x</sub>In<sub>1-x</sub>P építaxial.

*During the last decade a new method for the preparation of III-V binary compounds and ternary alloys using ultra high vacuum technology has been developed. This technique now known as Molecular Beam Epitaxy (MBE) is a refined form of vacuum evaporation. It allows films to be grown with precise control over chemical composition, crystal perfection and doping levels. This degree of control is achieved by supplying controlled amounts of material to the growth interface from molecular beam sources. This article discusses the technology required for MBE, the state of knowledge of processes which control the growth, composition and dopant incorporation and the properties of both homoepitaxial GaAs and multilayer epitaxial films of GaAs-Ga<sub>x</sub>In<sub>1-x</sub>P.*

**M**OLECULAR Beam Epitaxy (MBE) has received a considerable amount of attention over the last few years as a technique for the preparation of thin films of III-V binary compounds and alloys. Recent review articles have discussed the technology, growth processes and device applications [1-3]. MBE is a refined form of vacuum evaporation in which directed beams of atoms or molecules are condensed onto a heated substrate under ultra-high vacuum conditions. The particular merits of the technique are that thin films can be grown with precise control over thickness,

composition and doping level. The composition and dopant concentrations can be changed abruptly (within a few Å) or continuously permitting previously unobtainable structures to be prepared [4]. Material of device quality has been obtained in several laboratories and in the next few years the process seems likely to be used in a production environment for specialised devices.

This article describes the present state of development of MBE within the Philips Laboratories. Following a brief discussion of the technology of MBE the surface processes controlling growth and dopant incorporation are discussed. The electrical and photoluminescent properties of homoepitaxial GaAs layers are reported. A brief discussion of alloy film properties is also included.

\* C.T. Foxon, Philips Research Laboratories, Redhill, Surrey (England).

## THE TECHNOLOGY OF MOLECULAR BEAM EPITAXY

Figure 1 shows a typical MBE system which features a stainless steel UHV chamber, having a base pressure of  $\approx 10^{-7} \text{N}\cdot\text{m}^{-2}$ \* without bakeout or  $5 \times 10^{-9} \text{N}\cdot\text{m}^{-2}$  after bakeout, achieved either with an ion pump, or a suitably trapped diffusion pump. Additional pumping is provided by a liquid nitrogen cooled titanium sublimator and liquid nitrogen cooled cryo-panels. The important feature of the system, which makes it different from conventional vacuum evaporation, is that Knudsen effusion cells are used to produce atomic or molecular beams of the film constituents, which are directed at the heated substrate. The cells which have accurate temperature control to  $\pm 1 \text{ K}$ , are thermally isolated from each other, and the complete cell assembly is surrounded by a liquid nitrogen cooled shroud, which provides beam collimation, additional cryopumping and thermal isolation from the rest of the vacuum chamber to minimise outgassing.

If the cell contains vapour in equilibrium with the condensed phase, the flux,  $J$ , (expressed in  $\text{mol}\cdot\text{cm}^{-2}\cdot\text{s}^{-1}$ ), at the substrate is given by :

$$J = 1.11 \times 10^{22} [ap/d^2(MT)^{1/2}] \cos \theta \quad (1)$$

provided that the cell aperture is less than the mean free path of vapour molecules within the cell (i.e. the molecular flow region). In equation (1)  $a$  is the aperture area,  $p$  the vapour pressure in the cell,  $d$  the distance from aperture to substrate, and  $\theta$  the angle between the beam and the normal to the substrate,  $M$  the molecular weight of the beam molecules and  $T$  the absolute temperature of the source. Fluxes used are typically  $\approx 10^{16} \text{mol}\cdot\text{cm}^{-2}\cdot\text{s}^{-1}$  for group V elements,  $\approx 10^{15} \text{at}\cdot\text{cm}^{-2}\cdot\text{s}^{-1}$  for group III elements and  $10^9 - 10^{11} \text{at}\cdot\text{cm}^{-2}\cdot\text{s}^{-1}$  for dopants, produced with cell pressures of  $10^{-1} \text{N}\cdot\text{m}^{-2}$  for the main constituents and correspondingly lower for dopants. This gives growth rates of  $\approx 1 \mu\text{m}\cdot\text{h}^{-1}$ , and the fluxes can be very rapidly interrupted by a beam shutter. Substrates are mounted on an internally heated Mo block using a thin layer of liquid In (or Ga) to provide good thermal contact.

In a system used for film growth for device applications a number of monitoring devices are required. A beam monitoring ion gauge can be used to control beam fluxes to  $\pm 1 \%$ , allowing good control over the composition of ternary alloys such as  $\text{Ga}_x\text{In}_{1-x}\text{P}$ .

\*  $1 \text{ N}\cdot\text{m}^{-2} = 7.5 \times 10^{-3} \text{ torr}$ .

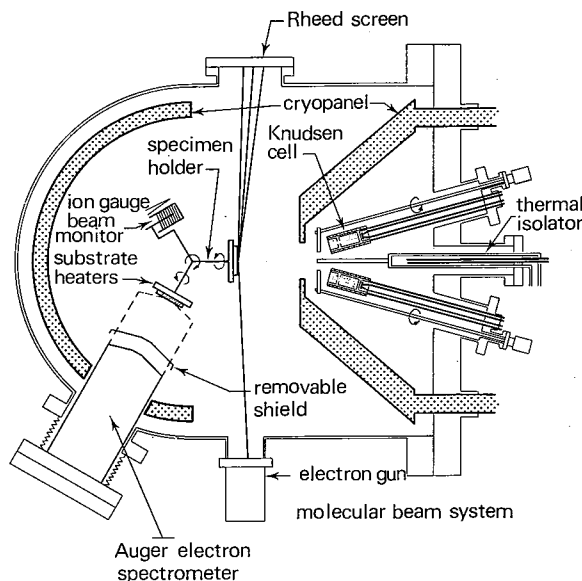


Fig. 1. Schematic diagram of a typical molecular beam epitaxy system.

The ion gauge may be calibrated by weighing a deposit or by measuring film thickness. A mass spectrometer may be employed to monitor the background gases present before and during epitaxy and may be used as an alternative to the ion gauge for beam monitoring purposes. A reflection electron diffraction facility is frequently used to monitor both substrate cleaning and to determine the surface structures present during growth. A surface analytical facility such as Auger Electron Spectroscopy (AES) can also be useful for monitoring the chemical composition of the surface before and after growth.

### Source materials

The source materials used to produce the beams may be either the group III and V elements, or the III-V compounds themselves. The compounds are used to produce the group V flux, an additional elemental source providing the appropriate intensity of group III material. Dopant beams are always generated from elemental sources, with so far Sn, Si, Ge, Mg, Mn and Be having been used with varying degrees of success to produce N-type (Sn, Si, Ge) and P-type (Mg, Mn, Be and Ge) films. In addition,  $\text{Zn}^+$  ion beams have been used to produce P-type films.

The flux from an elemental source of group V materials is always composed of the tetramer ( $\text{P}_4$ ,  $\text{As}_4$ ,  $\text{Sb}_4$ ), but when a III-V compound is used as the source of the group V element, principally dimers are produced. For example, from GaAs, the  $\text{As}_2/\text{As}_4$  ratio is  $> 10^4/1$ , as is the  $\text{P}_2/\text{P}_4$  ratio from GaP, while from InP it is approximately 10/1. All group III and dopant element beams are monoatomic.

### Substrate preparation and assessment

After some standard form of chemical or mechano-chemical polishing, e.g. bromine-methanol or lithium hypochlorite, the substrate is free etched in a 7:1:1 solution of  $H_2SO_4$ ,  $H_2O_2$ ,  $H_2O$  and washed in high purity water. At this stage the surface is hydrophobic and the substrate is mounted in the vacuum system. Surface analysis using AES usually shows that the surface is contaminated with both oxygen and a small amount of carbon (fig. 2, courbe a). The oxide is removed by heating the substrate within the congruent evaporation region in a flux of arsenic (typically  $10^{13}-10^{14} \text{ cm}^{-2}\cdot\text{s}^{-1}$ ). Auger analysis of the heated surface shows that the oxygen can be totally removed by this treatment but that in general a small amount of carbon is detected.

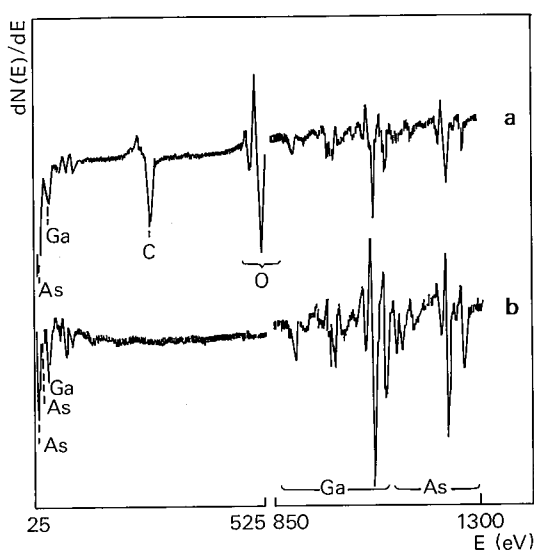


Fig. 2. Auger spectrum of a chemically prepared GaAs substrate (a) and a GaAs layer prepared by molecular beam epitaxy (b).

## SURFACE CHEMISTRY OF GROWTH PROCESSES

In this section we will consider first the experimental techniques which can be applied to determine the kinetics and mechanisms of growth processes, then summarize the results which have been obtained and finally discuss the models which have been proposed to account for the kinetic data. We will deal first with GaAs, and then show how this can be extended to alloy films.

### Experimental approach

Surface kinetic data on growth and doping can be obtained using modulated molecular beam techniques. In this method perturbation of an incident flux gives rise to a time varying concentration of adsorbed molecules on the substrate surface, and hence to a time dependent desorption rate, which can be measured mass spectrometrically. Alternatively, by modulating the desorption flux, atomic and molecular species which are leaving the surface directly can be identified and distinguished from background vapour species. In addition surface analytical techniques (AES, LEED, RHEED) permit detailed assessment to be made of substrate surfaces at any stage of a process, and, combined with temperature programmed thermal desorption provide information on surface stoichiometry.

An experimental system suitable for performing modulated molecular beam mass spectrometry studies, together with associated surface compositional analysis, is essentially similar to that used for film growth applications and similar beam sources are employed. Rotatable shutters driven by UHV compatible motors provide a periodic modulation of the incident and desorbing molecular beams. Ion counting and signal averaging techniques are used to acquire statistically significant data, and by Fourier transforming both the detected periodic signal and the known time dependence of the flux, the attenuation and phase shift of the Fourier components of this flux due to all processes between beam modulation and detection are obtained. The attenuation and phase shift caused by all events other than the surface processes of interest are then removed by deconvolution. The details of the method have been reported by C.T. Foxon et al. [6].

The kinetic information which can be extracted from modulated beam experiments is quite comprehensive. Firstly, surface lifetimes of adsorbed atoms or molecules can be determined directly, and when measured as a function of temperature enable desorption energies to be deduced. Secondly, sticking coefficients can also be measured directly, and it is therefore necessary to define these two important parameters, surface lifetime and sticking coefficient, in relation to the technique used to determine them. Where the lifetime of a trapped molecule is short compared to the modulation frequency, it may be considered to be scattered either elastically or inelastically, but where the lifetime becomes very long the molecule is chemisorbed. The sticking coefficient can then be unambiguously defined as that fraction of incident molecules which is finally chemisorbed. In practical terms the minimum modulation frequency is 0.5 Hz, so that surface lifetimes  $\gg 1 \text{ s}$  would correspond to chemisorption. Orders of chemical reactions can also be determined, and this is an essential feature in the modelling of surface processes. By modulating the desorption flux additional information can be obtained, in that desorbing species can be unequivocally identified as originating from the surface, and desorption rates can be measured directly.

### Kinetics of film growth for III-V compounds

We will confine our discussion to the autoepitaxial growth of GaAs on (100) oriented GaAs substrates, but other III-V compounds behave almost identically. There are two procedures which may be used for the preparation of GaAs films by MBE. One uses beams of  $\text{As}_4$  (derived from an arsenic source) and Ga, while the other uses  $\text{As}_2$  (from a GaAs source) and Ga, which in each system impinge on a heated substrate where interaction occurs. The chemistry of both surface reactions has been investigated in detail [7, 8] and although there are substantial differences between them, kinetic models fully consistent with the experimental data can be formulated for each system.

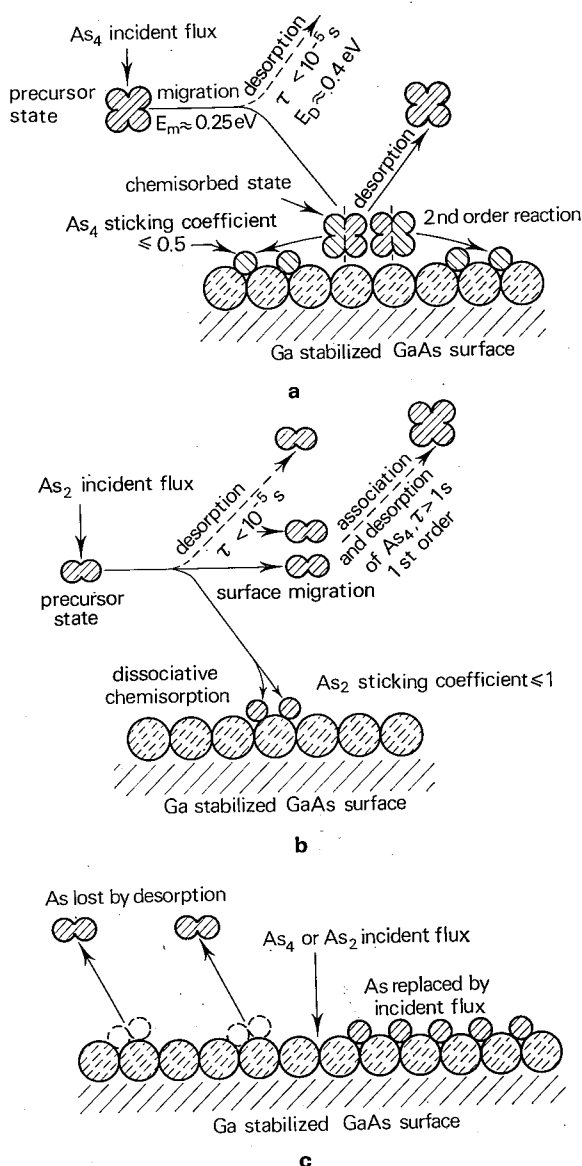


Fig. 3. Growth models for GaAs.

- a Growth from Ga and  $\text{As}_4$  below 600 K.  
 b Growth from Ga and  $\text{As}_2$  below 600 K.  
 c Growth above 600 K.

### $\text{Ga-As}_4$ interaction kinetics on (100) GaAs surfaces below 600 K

The important features of the model are illustrated in figure 3a.  $\text{As}_4$  is adsorbed into a mobile precursor state and in the absence of a surface Ga population has a zero sticking coefficient, but a measurable surface lifetime in the temperature range 300-450 K.

From the temperature dependence of the lifetime a desorption energy of  $\approx 0.4$  eV may be determined. With a coincident Ga flux,  $\text{As}_4$  has a temperature independent sticking coefficient between 450 and 600 K, but it is a function of the Ga beam intensity,  $J_{\text{Ga}}$ . The crucial results are that the sticking coefficient of  $\text{As}_4$ ,  $S_{\text{As}_4}$ , is always  $\leq 0.5$ , even when  $J_{\text{Ga}} \gg J_{\text{As}_4}$  (the  $\text{As}_4$  flux); secondly, when  $J_{\text{Ga}} \ll J_{\text{As}_4}$ , one As atom sticks for every Ga atom supplied; and finally, when  $J_{\text{Ga}} \gg J_{\text{As}_4}$ , the desorption rate of  $\text{As}_4$  is second order with respect to its adsorption rate, but for  $J_{\text{Ga}} \ll J_{\text{As}_4}$  a first order dependence is observed.

These results can be explained by a process of dissociative chemisorption, with a pairwise interaction of  $\text{As}_4$  molecules adsorbed on adjacent Ga lattice sites. When the  $\text{As}_4$  surface population is small compared to the number of Ga sites the rate limiting step is the encounter/reaction probability between  $\text{As}_4$  molecules leading to second order kinetics. As the  $\text{As}_4$  surface population is increased, there is an increasing probability that an arriving molecule will find adjacent sites occupied and the desorption rate becomes proportional to the number of molecules being supplied, i.e. a first order process.

It will be useful at this stage to introduce the concept of Ga and As stabilized surfaces, first discussed by A.Y. Cho [9, 10]. LEED and RHEED observations showed that at least two structures could exist on (111)B and (100) surfaces, and that a particular structure was stable with respect to a specific temperature and the relative arrival rates of gallium and arsenic at the surface. For example, on a (100) surface the two principle structures which are stable over fairly wide temperature and flux ranges are the  $\text{GaAs}(100)-(2 \times 4)$  or  $\text{C}(2 \times 8)$  As-stable surface, which occurs when  $J_{\text{As}_4} > J_{\text{Ga}}$ , i.e. when  $S_{\text{As}_4} < 0.5$ , and the  $(4 \times 2)$  or  $\text{C}(8 \times 2)$  Ga-stable structure, observed when  $2J_{\text{Ga}} > J_{\text{As}_4}$  and  $S_{\text{As}_4} = 0.5$ .

### $\text{Ga-As}_2$ interaction kinetics on (100) GaAs surfaces below 600 K

The second approach to the growth of GaAs by MBE is to use beams of Ga and  $\text{As}_2$  (from a GaAs source), and the interaction kinetic model for these two species on a (100) GaAs surface is represented schematically in figure 3b. At 600 K the sticking coefficient of  $\text{As}_2$ ,  $S_{\text{As}_2}$ , is a function of the arrival rate of Ga, and when  $J_{\text{Ga}} < J_{\text{As}_2}$  one As atom sticks for each Ga atom supplied, while for  $2J_{\text{Ga}} \geq J_{\text{As}_2}$ ,  $S_{\text{As}_2}$  is unity (cf.  $S_{\text{As}_4} = 0.5$  for the equivalent situation). Below 600 K, the behaviour of  $\text{As}_2$  becomes more complex, in that it undergoes a surface association

reaction, leading to the desorption of  $As_4$ , by a first order process with respect to  $J_{As_2}$ .

#### *Interactions on GaAs surfaces above 600 K*

At substrate temperatures above 600 K an additional process occurs which is illustrated in figure 3c.  $As_2$  is lost by desorption from the GaAs surface at a rate which increases with increasing temperature. This desorption process creates a Ga adatom population and in the absence of an impinging arsenic flux results in a *Ga-stable* structure being established. In the limit free gallium may be produced on the surface.  $As_2$  lost in this way from the surface may be replaced by dissociation of incident  $As_2$  or  $As_4$  beams to maintain an *As-stabilized* structure providing the arsenic supply rate exceeds rate of loss of  $As_2$  by thermal desorption. The flux ratio  $J_{As_4}$  to  $J_{Ga}$  required to maintain a specific surface structure during growth will therefore depend upon the substrate temperature and the absolute magnitude of the fluxes.

#### **Kinetic processes in the growth of $Ga_xIn_{1-x}As(P)$ alloys**

Perhaps the most critical factor in alloy film growth by MBE is to produce material whose composition is homogeneous and related in a comparatively simple way to the incident fluxes. We have established [11] that for the growth of III-III-V ternary alloys two surface processes can occur which seriously impair compositional uniformity and control. These are respectively preferential desorption of the group V element, and, at some higher temperature, preferential desorption of one of the group III elements. If we consider first the desorption of the group V element, results indicate that in this respect the alloy may simply be considered as a mixture of the two binary compounds of which it is composed, i.e. InAs and GaAs in the case of  $Ga_xIn_{1-x}As$ .  $As_2$  then desorbs above 550 K to leave a surface with an enriched In and Ga adatom population. In principle this loss by desorption could be balanced by increasing the incident  $As_4$  flux, but in practice, as the temperature is increased the required flux becomes impracticably high. This is especially true for GaInAs and GaInP. AES results conclusively demonstrate that provided growth is carried out at temperatures below which InAs (or InP in the case of  $Ga_xIn_{1-x}P$ ) are thermally stable, the surface composition of the alloy reflects the relative flux intensities of Ga and In.

The preferential desorption of  $As_2$ , which increases with increasing temperature, leads to a temperature dependent sticking coefficient of  $As_4$ , but it is important to note that in agreement with the previous model for GaAs,  $S_{As_4}$  never exceeds 0.5, and in fact this limiting value is only reached when the surface has reconstructed to the group III element stable form. These conditions presumably correspond to the maximum number of surface atoms possible before the free metal begins to form on the surface. At somewhat higher temperatures ( $> 700$  K), In can desorb from the surface of  $Ga_xIn_{1-x}As$  (P)

during growth. In the case of  $Ga_xIn_{1-x}As$  the desorption energy is 1.5 eV, which is 1 eV lower than the heat of vapourization of In.

We can conclude, therefore, that the principle limitation to the growth of III-III-V alloy films by MBE is simply the thermal stability of the less stable of the two III-V compounds of which the alloy may be considered to be composed. In addition, preferential desorption of the more volatile group III element can occur at higher temperatures.

## GROWTH OF

## HOMOEPITAXIAL GaAs

For the work discussed in this section we have exploited the technique of reflection high energy electron diffraction (RHEED) to monitor continuously the surface of the growing film. We shall be particularly concerned with the temperature range for growth of autoepitaxial films of GaAs, surface reconstruction effects observed during growth, and the electrical and optical properties of such films.

#### **Temperature range for growth of MBE GaAs**

An evaluation of the kinetics of surface reactions involved in the growth of GaAs films on (100) GaAs substrates from molecular beams of Ga and  $As_4$  [7] suggests that GaAs should be formed at substrate temperature at least as low as 450 K. The chemical limitation occurs at the point where the adsorption of  $As_4$  molecules becomes non-dissociative, but the experimental technique used in the kinetic measurements, modulated molecular beam mass spectrometry, does not provide any structural information.

The range of growth temperatures over which single crystal films are obtained as reported in the literature is rather wide, with no real consensus of opinion between different authors. However, minimum temperatures quoted are all substantially above the fundamental limit predicted by the surface chemistry.

From a systematic study of substrate temperature effects using RHEED [12], the results of which are shown in figure 4, it has been possible to establish that provided the substrate surface on which growth commences is sufficiently clean and perfect, autoepitaxial GaAs films which maintain a reconstructed, atomically smooth surface can be grown from  $\approx 870$  to  $\approx 530$  K, and from  $\approx 530$  to  $\approx 365$  K smooth single crystal films showing a bulk surface structure can be prepared. In the narrow temperature range 365-345 K, although the growth is still epitaxial, the

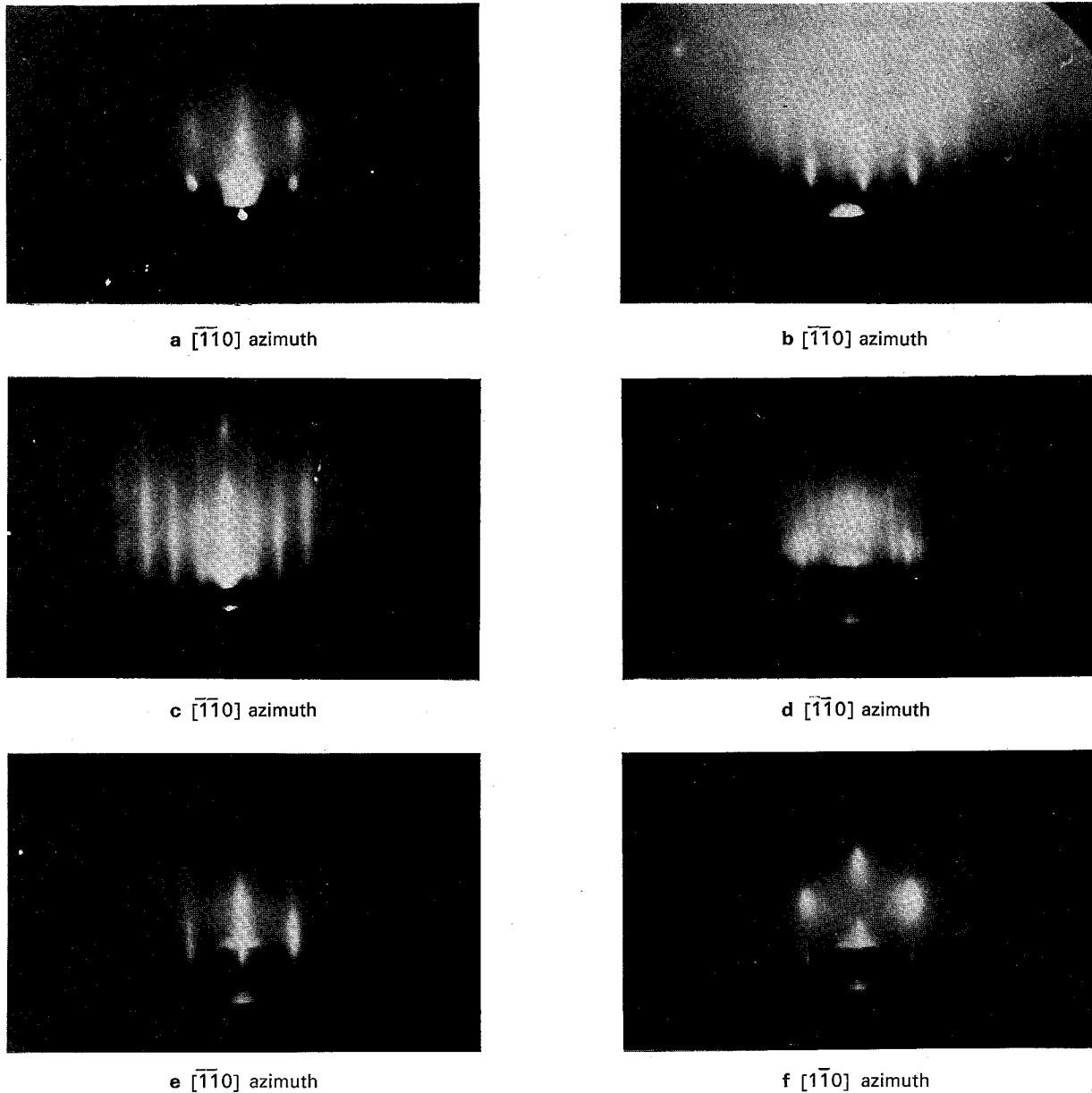


**Fig. 4.** Rheed patterns, 3 keV primary energy azimuth as shown.

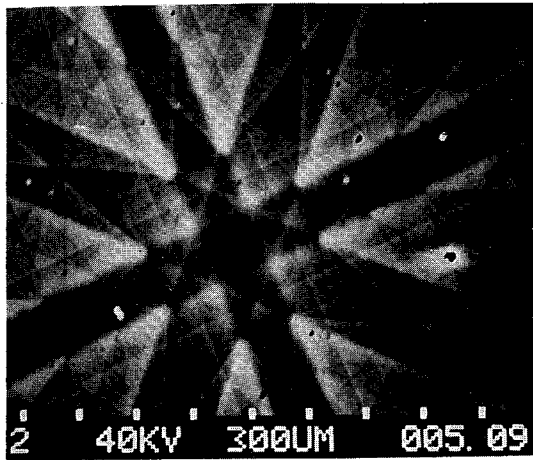
- a Surface after initial heat treatment in an  $\text{As}_4$  flux.
- b Prolonged heat treatment in  $\text{As}_4$ .
- c, d Grown surface, showing As-stable reconstruction, two orthogonal  $\langle 110 \rangle$  azimuths. Substrate temperature:  $T_s > 620$  K.
- e Grown surface, with only bulk rods visible,  $620 \text{ K} > T_s > 530$  K.
- f Grown surface,  $T_s \approx 365$  K.

diffraction patterns indicate that some surface roughening is occurring, in that rods are replaced by spots while the side band arcs may arise from surface steps. Below 345 K only an amorphous surface layer can be detected.

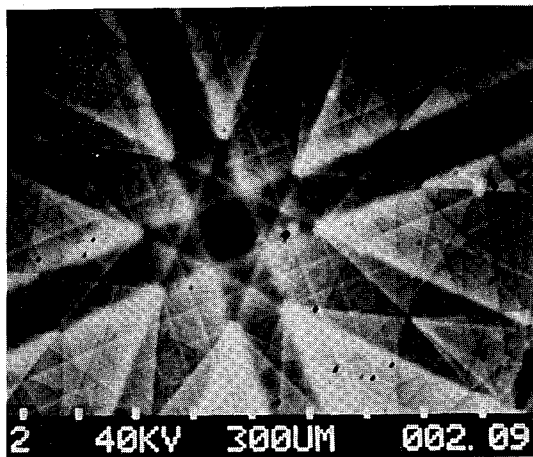
We have obtained a qualitative assessment of the crystal perfection of a film grown at 370 K from electron channelling micrographs taken in the specimen current mode. A typical micrograph is shown

in figure 5a, and for comparison figure 5b is a corresponding micrograph from a film grown at 790 K.

With this technique, as perfection decreases, the contrast decreases and the line widths increase, so that higher order (narrower) lines progressively disappear. It is apparent from careful inspection of figures 5a and 5b that while there are minor differences, the perfection has not been significantly degraded by the very low temperature.



a



b

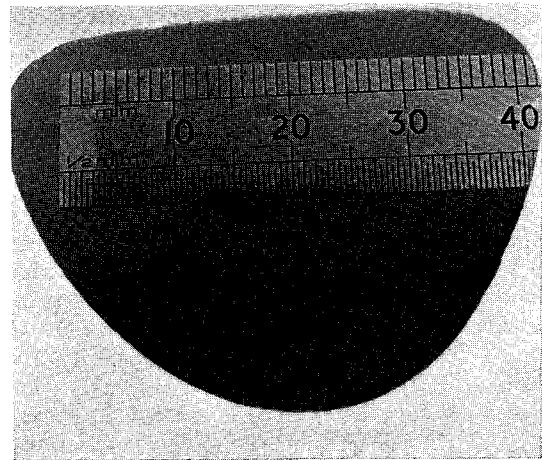
**Fig. 5.** Electron channelling micrographs obtained in the specimen current mode.

- a Film grown at 370 K, thickness  $\approx 0.2 \mu\text{m}$ .  
 b Film grown at 790 K, thickness  $\approx 1.0 \mu\text{m}$ .

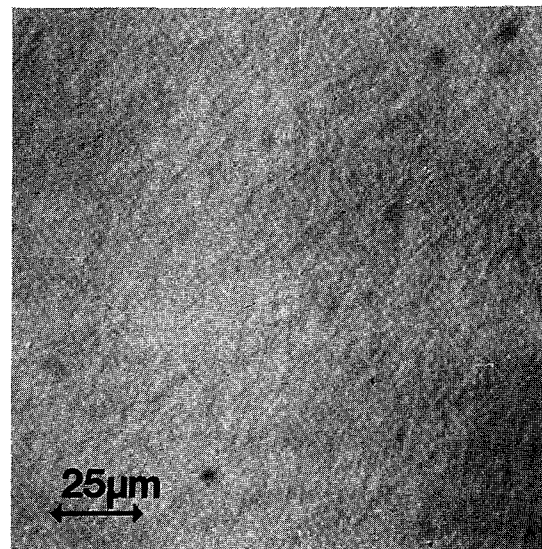
### Surface topography and crystal perfection of MBE GaAs

One of the major advantages of material grown by MBE is the quality of the surface topography on all scales from macroscopic to microscopic. This is in general true for all low index orientations and for crystals grown a few degrees *off orientation*. The exceptions to this rule occur when growing on a highly contaminated surface or when growing under excess gallium (or group III) conditions, i.e. with more Ga to As<sub>4</sub> arriving than is required to produce a gallium stable surface reconstruction during growth.

Figure 6a shows a macroscopic view of the surface of a GaAs autoepitaxial film grown on a (100) surface. Figure 6b shows a Nomarski interference micrograph of part of the same sample at higher magnification. Growth of autoepitaxial GaAs by MBE appears to proceed in a two dimensional manner by



a



b

**Fig. 6.** GaAs autoepitaxial film grown on a (100) surface by molecular beam epitaxy.

- a Macroscopic view of the surface.  
 b Nomarski interference micrograph of part of the same sample ( $\times 400$ ).

the propagation of steps across the surface. The contrast which is observed when growing on a contaminated substrate occurs because the horizontal propagation of steps is impeded and a three dimensional growth mode is observed.

Examination of autoepitaxial films and of the layer substrate interface in the transmission electron microscope has shown that for films grown above 670 K no defects other than those propagating from the substrate are present. A low concentration of defect clusters ( $\approx 10^5 \text{cm}^{-2}$  in a foil  $\approx 1000 \text{ \AA}$  thick) is observed when growing at lower temperatures, however. The origin and nature of such clusters is not at present understood, but work is currently in progress to identify and eliminate them.

### Background impurities in MBE grown material

Whilst it is impossible to give a single figure for the background impurities present in undoped films grown by MBE, it is now possible to give a general guide based on the known long term performance of four growth systems. Films of GaAs grown above 700 K are usually compensated P-type with hole mobilities which suggest a total impurity content of  $N_A + N_D \leq 10^{16} \text{ cm}^{-3}$ . Depending upon the degree of compensation free carrier concentrations can be as low as  $10^{12} \text{ cm}^{-3}$  but are usually between  $10^{14} - 10^{15} \text{ cm}^{-3}$ . The identification of background impurities is discussed below.

### Growth of doped films

To evaluate the mechanisms involved in producing doped films, two processes must be understood. The first is the interaction behaviour of the dopant with a GaAs surface, especially in the presence of larger fluxes of Ga and  $\text{As}_4$  (or  $\text{As}_2$ ); the second is the incorporation and extent of electrical activity of the dopant in the growing film.

In practice, all materials which have been used successfully as dopants have unity sticking coefficients (as measured by modulated beam techniques) over the whole range of growth conditions. Useful N-type dopants include Sn, Ge and Si, while for P-type doping Be and Mn have given satisfactory results, although the Mn acceptor level is rather deep ( $\approx 100 \text{ meV}$ ), and Mn also disturbs growth morphology at concentrations  $> 10^{18} \text{ cm}^{-3}$  [13].

Of other potential dopants, Zn and Cd show complex surface interaction behaviour [14], and have zero sticking coefficients at substrate temperatures  $> 370 \text{ K}$ . Pb has a unity sticking coefficient at 300 K, but desorbs in the temperature range 500-700 K with a desorption energy of  $\approx 2 \text{ eV}$  following first order kinetics. Te has a sticking coefficient close to unity for submonolayer concentrations over a wide temperature range, but displaces arsenic from an arsenic stabilised structure, presumably by forming the stable compound  $\text{GaTe}$ . Consequently it becomes strongly segregated in the surface and is unsuitable as a dopant [15]. Mg has a unity sticking coefficient [16] but only one incident atom in  $10^5$  is electrically active [17]; the reason for this low level of activity is not known.

We will consider in rather more detail three dopants, Be, Sn and Ge, each of which illustrates different factors which must be considered when producing doped films.

#### Beryllium

Be behaves as an almost ideal P-type dopant in autoepitaxial films of GaAs prepared by MBE.

Figure 7 shows measured and calculated values of free acceptor concentration as a function of Be cell

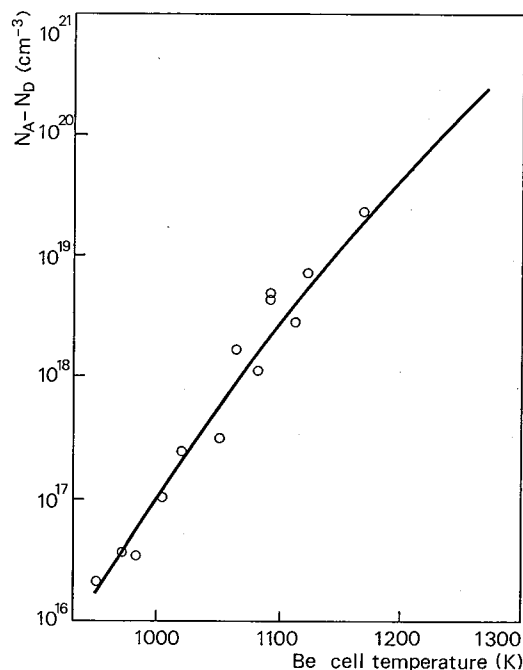


Fig. 7. Free acceptor concentration as a function of Be cell temperature.

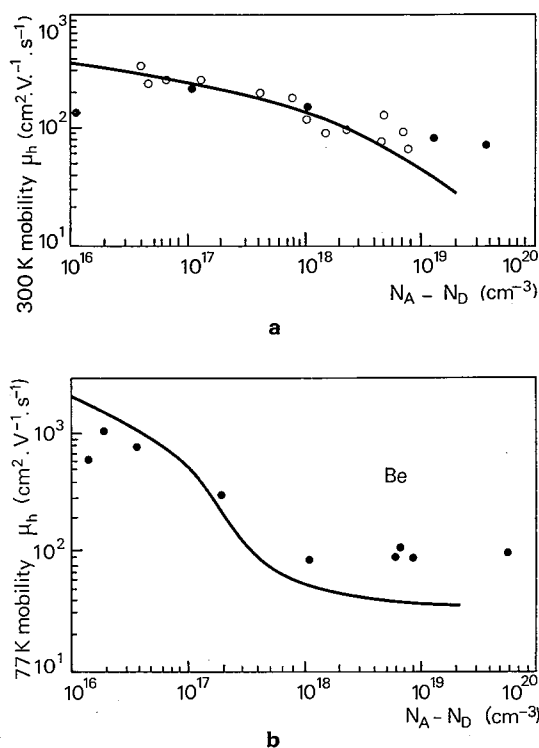


Fig. 8. Hole mobility as a function of acceptor concentration, solid curves representing optimum published data.

a at 300 K; b at 77 K.

temperature, and it is clear that the agreement is excellent over a wide range. This means that one incident Be atom produces one free acceptor; there is no evidence for the incorporation of Be in any other form. In addition, doping profiles are completely



flat, and hole mobilities at 300 and 77 K as a function of free acceptor concentrations follow very closely curves drawn through optimum published data (figures 8a and 8b). Other results for Be-doping in MBE have been published by M. Ilegems [18].

### Tin

The important feature of Sn doping is that there is a surface rate limitation to its incorporation, so that until a steady state surface population is formed, which can be as large as 0.1 monolayer, the free donor density is not constant, but increases asymptotically to a steady state value. The rate constant associated with this process is strongly dependent on the  $\text{As}_4$  flux, and to a lesser extent on substrate temperature. At constant growth rate (Ga flux constant) and constant Sn flux, therefore, transients are observed in the free donor concentration at the beginning of growth, or where the  $\text{As}_4$  flux or substrate temperature are changed during growth. This is illustrated in figure 9 which shows C-V measured free carrier profiles under various growth conditions. Curve a corresponds to growth at low  $\text{As}_4$  to Ga flux ratios where the rate constant for incorporation is low. Consequently until a relatively large surface concentration is established the incorporation rate of Sn is less than the supply rate and loss of free carriers is observed at the interface. Auger analysis of the surface of GaAs films grown under such conditions shows the presence of a surface concentration of tin approximately equal to the total number of free donors missing at the interface. Increasing the  $\text{As}_4$  to Ga flux ratio increases the incorporation rate and here steady state is achieved more rapidly with a smaller loss of free carriers at the interface (fig. 9, curve b). The observed loss may be removed entirely by predepositing tin which effectively builds up the steady state surface concentration of Sn required to make the incorporation rate equal the supply rate (fig. 9, curve c). Away from

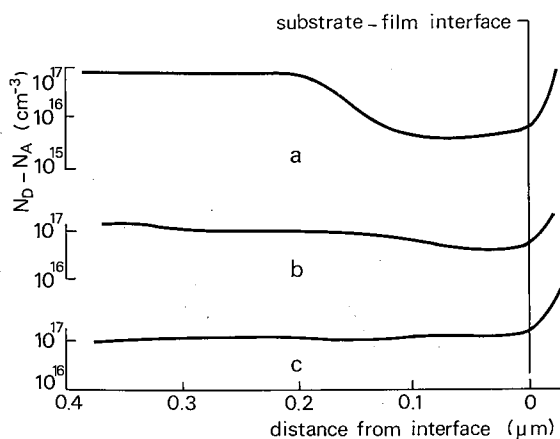


Fig. 9. C-V profiles of Sn doped GaAs layers grown on  $\text{N}^+$  substrates at 755 K.

Curve a  $J_{\text{As}_4} = 2 \times 10^{14} \text{ mol} \cdot \text{cm}^{-2} \cdot \text{s}^{-1}$ ; curve b  $J_{\text{As}_4} = 2 \times 10^{16} \text{ mol} \cdot \text{cm}^{-2} \cdot \text{s}^{-1}$ ; curve c  $J_{\text{As}_4} = 2 \times 10^{16} \text{ mol} \cdot \text{cm}^{-2} \cdot \text{s}^{-1}$  with  $3 \times 10^{12} \text{ Sn} \cdot \text{cm}^{-2}$  deposited prior to growth.

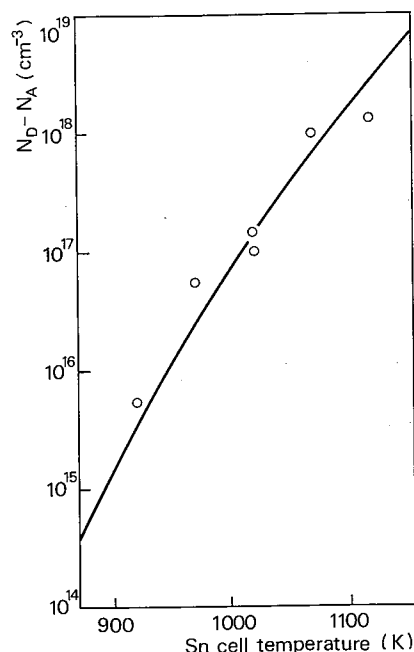
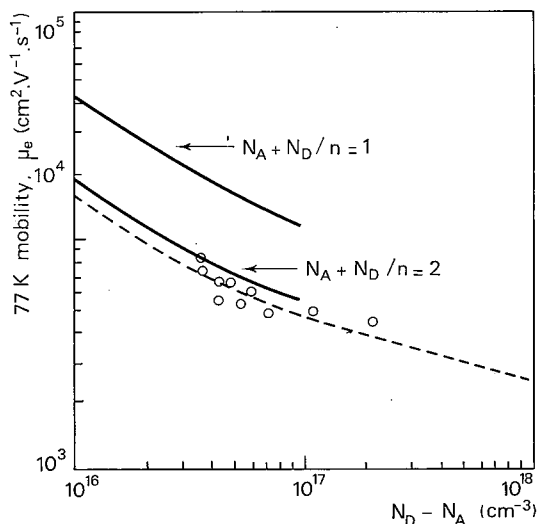
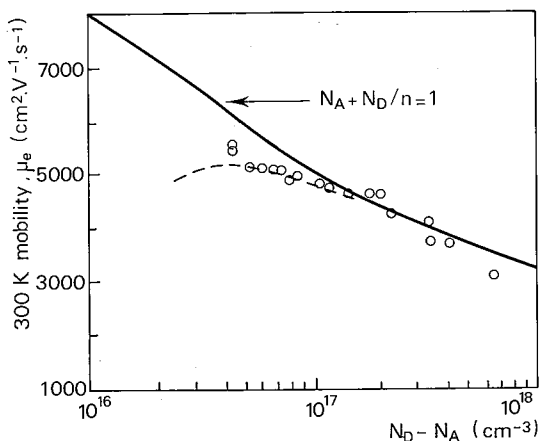


Fig. 10. Free donor concentration as a function of Sn cell temperature.

the interface under all constant conditions of growth, the steady state free donor doping profiles are flat with a free donor concentration proportional to the Sn flux as shown in figure 10; the free carrier concentration is equal to the chemical composition. Electron mobilities at 300 and 77 K as a function of free donor concentration are close to theoretical assuming a background acceptor concentration of  $10^{16} \text{ cm}^{-3}$  (see fig. 11a et 11b). There is no evidence for Sn being incorporated onto an acceptor site.

### Germanium

The important aspect of doping with Ge is that it is amphoteric, and that the relative proportions incorporated onto donor and acceptor sites are a function of growth conditions [19]. This effect is illustrated in figure 12 for Ge doped GaAs layers grown by MBE. The total Ge content in the layer  $N_D + N_A$  is calculated from the Ge flux and the free carrier concentration  $N_D - N_A$  is deduced from C-V profiles; there is an approximately linear relation between the ratios  $(N_D/N_A)$  and  $(J_{\text{As}_4}/J_{\text{Ga}})$ . This suggests that the probability of incorporation into a donor or acceptor site may be proportional to the number of vacancies of the appropriate type. Figure 13 shows the relation between the free carrier concentration and Ge cell temperature for films grown at a constant temperature and with a constant flux ratio of  $\text{As}_4$  to Ga. Due to auto-compensation in Ge doped films the data do not follow the theoretical curve but are displaced. Also shown in figure 13 is the calculated total Ge concentration assuming a constant ratio  $(N_D/N_A)_{\text{Ge}} = 3.0$  and a background acceptor concentration of  $\approx 0.6 \times 10^{16} \text{ cm}^{-3}$ ; there is excellent agreement



**Fig. 11.** Electron mobility as a function of donor concentrations, solid curves representing optimum published data.

a at 300 K; — theory from Rode and Knight, ... theoretical curve for constant  $N_A = 1.0 \times 10^{16} \text{ cm}^{-3}$ . b at 77 K; — theory from Rode and Knight, ... empiric curve from Poth et al.

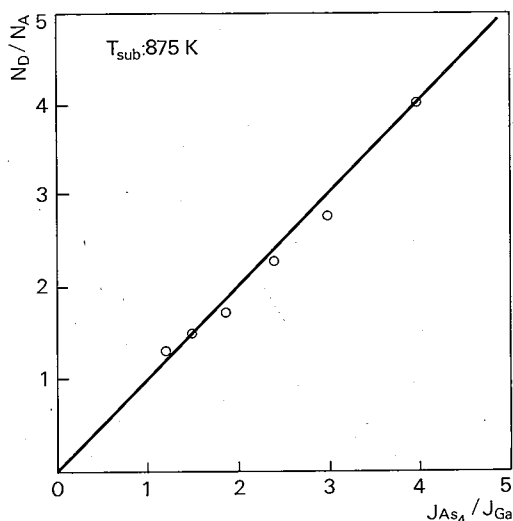


**Fig. 12.**  $(N_D/N_A)_{Ge}$  as a function of  $J_{As_4}/J_{Ga}$  ratio for GaAs films grown by molecular beam epitaxy.

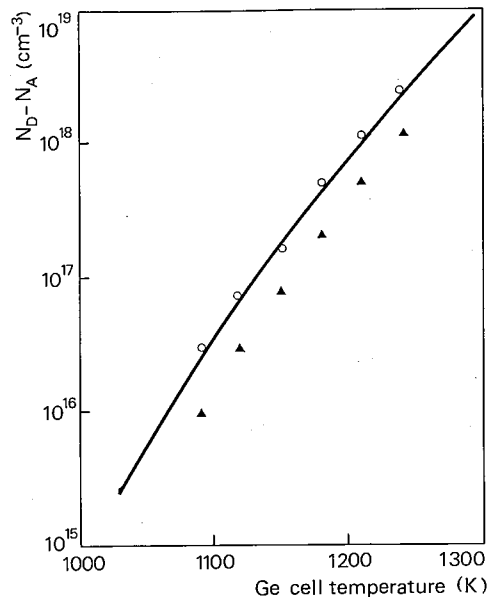


**Fig. 13.** Free donor concentration and calculated total Ge concentration as a function of Ge cell temperature.

▲: measured  $N_D - N_A$ ; ○: calculated  $[Ge]$  using  $(N_D/N_A)_{Ge} = 3$  and  $N_A$  (background)  $6 \times 10^{15} \text{ cm}^{-3}$ ; —  $[Ge]$  calculated from Ge cell temperature.

between the deduced values and the calculated curve. This also suggests that the total background doping level is  $\approx 10^{16} \text{ cm}^{-3}$  in good agreement with our previous observation (p. 146).

From the above data it is clear that P-type and N-type dopants exist for use in MBE and that doping concentrations in the range  $10^{16} - 3 \times 10^{19} \text{ cm}^{-3}$  can be achieved.

**Deep levels and residual impurities in MBE GaAs**

Deep levels in N-type MBE GaAs are being studied by Schottky barrier capacitance measurements using the Deep Level Transient Spectroscopy (DLTS) technique [20, 21]. In layers grown at 870 K three levels are commonly observed which probably correspond to levels M1, M3 and M4 reported by D.V. Lang et al. [22] in material grown under similar conditions. The lowest trap concentrations have been observed in Ge doped layers where as low as  $10^{-3}$  of the doping level have been measured, corresponding to volume concentrations  $\approx 3 \times 10^{13} \text{ cm}^{-3}$  [23].

**Photoluminescence in MBE GaAs**

The photoluminescence of homoepitaxial layers of GaAs grown by MBE has also been used to assess the presence of background contaminants in both undoped and doped films. For such measurements the sample is cooled to near liquid helium temperatures and electron-hole pairs created by irradiation with a krypton laser at a wavelength of 482.5 nm. The emission

from the sample is passed through a spectrometer to give a plot of photoluminescence v. wavelength. The position of the peaks can be used to identify the nature of the centre and the peak height used as a semi-quantitative measure of the concentration. Typical spectra for undoped, N-type and P-type films are shown in figure 14a, 14b, 14c respectively. From these

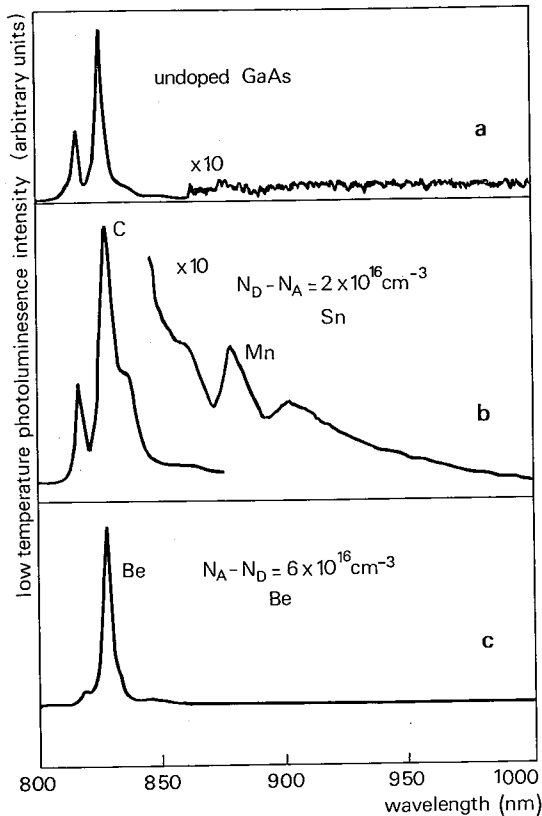


Fig. 14. Low temperature photoluminescence spectra from GaAs grown by molecular beam epitaxy.

a GaAs undoped ; b Sn doped ; c Be doped.

it can be seen that carbon is a commonly present shallow acceptor and that manganese is also observed under some conditions. The relative heights of Be and C can be used to estimate the carbon concentration which is  $\approx 10^{16} \text{ cm}^{-3}$ . This is in good agreement with estimates of background doping levels based on mobility figures for P-type undoped films quoted above.

The photoluminescence measured at room temperature where the dopant atoms are fully ionised can be used to assess the ideality of the dopants used in MBE material. To a first approximation the photon yield should be directly proportional to the product of the initial and final density of states for the electrons involved in the emission process. For both N and P type material therefore a linear dependence of photoluminescence on doping level is to be expected. Such behaviour is observed for both Sn and Be over a large part of the available doping range.

## MULTILAYER FILMS GROWN

### BY MOLECULAR BEAM EPITAXY

Whilst homoepitaxial films of GaAs are suitable for microwave device applications, optoelectronic devices require epitaxial alloy films in order to provide materials of different band gap and hence refractive index. In such structures the lattice parameter of the various epitaxial layers must be similar in order to avoid elastic strain or misfit induced defects. These specific features are to be found in the  $\text{GaAs}-\text{Ga}_x\text{In}_{1-x}\text{P}$  system where  $x = 0.51$ .

The kinetic work described p. 143 above indicated that an upper limit to the growth temperature for  $(\text{Ga}, \text{In})\text{P}$  was  $\approx 650 \text{ K}$ , whilst GaAs films can be grown at much higher temperature ( $\approx 900 \text{ K}$ ). Complex sandwich structures of the type shown in figure 15 can be grown sequentially with the substrate temperature being adjusted accordingly. The composition of the various epitaxial layers has been measured in two ways. X ray diffractometer measurements can be used to estimate the lattice parameter of the layers, and Vegard's law used to estimate the composition knowing the lattice parameters for the binary compounds. In such a multi component structure, however, the films are elastically strained and in general the relaxed lattice constant must be deduced from a knowledge of the elastic constants of the materials and their thermal expansion coefficients. The composition deduced from the X-ray data can be confirmed by direct measurement using Rutherford Back-Scattering (RBS).

In this technique the energy spectrum of  $\alpha$ -particles backscattered from a collimated monoenergetic beam incident on the surface gives information on composition as a function of depth. This method has been used to determine the chemical composition

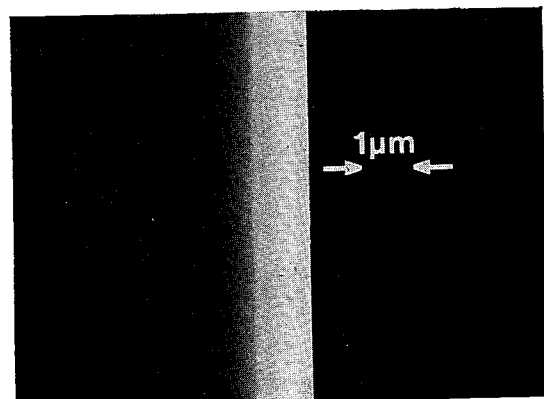


Fig. 15. Scanning electron micrograph of the cleaved edge of a multilayer film grown by molecular beam epitaxy.

and thickness of the upper (Ga, In)P and GaAs layers of the sandwich shown in figure 15. These values agreed well with those determined from X-ray data and with values deduced from a knowledge of the cell temperatures and system geometry.

Photoluminescence and interference techniques have also been used to determine the chemical composition, homogeneity and interface properties of such complex sandwich structures. From these measurements we have found there is no evidence for inter-diffusion between the various layers in the example shown in figure 15. The  $\text{Ga}_x\text{In}_{1-x}\text{P}$  grown at 650 K is electrically active and can be doped N-type and P-type in the range  $10^{18} - 3 \times 10^{19} \text{ cm}^{-3}$ , with corresponding photoluminescent properties.

Further studies of the electrical and optical properties of ternary alloys are currently being undertaken.

### CONCLUSION

Molecular Beam Epitaxy is now a well established growth technique within the Philips Laboratories. The basic mechanisms controlling the growth of binary III-V compounds and alloy films are well understood. Dopant incorporation has also been studied and P and N type films can be obtained in the range  $10^{16} - 10^{19} \text{ cm}^{-3}$ . However, further work is required to understand the mechanisms involved. Background impurities are  $\leq 10^{16} \text{ cm}^{-3}$  and deep level concentrations  $\leq 10^{13} \text{ cm}^{-3}$  can be achieved. Doped multilayer epitaxial films can be grown with good control over the composition and interfacial properties. Further research is required to obtain device quality material in this area.

The author is indebted to his colleagues for supplying details of the following material prior to publication elsewhere: to Dr. C.E.C. Wood for details of the behaviour of Sn and Ge as N type dopants, to Dr. J.S. Roberts for work relating to Be doping and multilayer structures, to Dr. P. Blood for information concerning deep level and Rutherford back scattering measurements and to Dr. G.B. Scott for data on the photoluminescence of both compound and alloy films.

- 1 CHO (A.Y.), ARTHUR (J.R.). — Molecular beam epitaxy. *Prog. Solid State Chem.*, **10**, (1975), 157-191.
- 2 CHANG (L.L.), ESAKI (L.), HOWARD (W.E.), LUDEKE (R.), SCHUL (G.). — Structures grown by molecular beam epitaxy. *J. Vac. Sci. & Technol.*, **10**, (1973), 655-662.

- 3 JOYCE (B.A.), FOXON (C.T.). — Kinetic studies of the growth of III-V compound using modulated molecular beam techniques. *J. Cryst. Growth*, **31**, (1975), 122-129.
- 4 ESAKI (L.), CHANG (L.L.). — New transport phenomena in a semiconductor superlattice. *Phys. Rev. Lett.*, **33**, (1974), 495-498.
- 5 FOXON (C.T.), JOYCE (B.A.), FARROW (R.F.C.), GRIFFITHS (R.M.). — The identification of species evolved in the evaporation of III-V compounds. *J. Phys. D*, **7**, (1974), 2422-2435.
- 6 FOXON (C.T.), BOUDRY (M.R.), JOYCE (B.A.). — Evaluation of surface kinetic data by the transform analysis of modulated molecular beam measurements. *Surf. Sci.*, **44**, (1974), 69-92.
- 7 FOXON (C.T.), JOYCE (B.A.). — Interaction kinetics of  $\text{As}_4$  and Ga on (100) GaAs surface using a modulated molecular beam technique. *Surf. Sci.*, **50**, (1975), 434-450.
- 8 FOXON (C.T.), JOYCE (B.A.). — Interaction kinetics of  $\text{As}_2$  and Ga on (100) GaAs surfaces. *Surf. Sci.*, **64**, (1977), 293-304.
- 9 CHO (A.Y.). — Morphology of epitaxial growth of gallium arsenide by a molecular beam method: the observation of surface structures. *J. Appl. Phys.*, **41**, (1970), 2780-2786.
- 10 CHO (A.Y.). — Gallium arsenide epitaxy by a molecular beam method: observations of surface structure on the (001) face. *J. Appl. Phys.*, **42**, (1971), 2074-2081.
- 11 FOXON (C.T.), JOYCE (B.A.). — Surface processes controlling the growth of  $\text{Ga}_x\text{In}_{1-x}\text{As}$  and  $\text{Ga}_x\text{In}_{1-x}\text{P}$  alloy films by molecular beam epitaxy. *J. Cryst. Growth*, **44**, (1978), 75-83.
- 12 NEAVE (J.H.), JOYCE (B.A.). — Structure and stoichiometry of (100) GaAs surfaces during molecular beam epitaxy. *J. Cryst. Growth*, **44**, (1978), 387-397.
- 13 ILEGEMS (M.), DINGLE (R.). — Acceptor incorporation in GaAs grown by molecular beam epitaxy. *Proc. 5 th Int. Symp. on GaAs and related compounds*, Deauville, (1974), London, Inst. Phys. ed., conf. ser. n° 24, (1975), 1-9.
- 14 LAURENCE (G.), JOYCE (B.A.), FOXON (C.T.), JANSSEN (A.P.), SAMUEL (G.S.), VENABLES (J.A.). — Adsorption-desorption studies of Zn in GaAs. *Surf. Sci.*, **68**, (1977), 190-203.
- 15 ARTHUR (J.R.). — Surface stoichiometry and structure of GaAs. *Surf. Sci.*, **43**, (1974), 449-461.
- 16 JOYCE (B.A.), FOXON (C.T.). — Growth and doping kinetics in molecular beam epitaxy. *Jap. J. Appl. Phys.*, **16**, (1977), 17-23.
- 17 CHO (A.Y.), PANISH (M.B.). — Magnesium doped GaAs and  $\text{Al}_x\text{Ga}_{1-x}\text{As}$  by molecular beam epitaxy. *J. Appl. Phys.*, **43**, (1972), 5118-5123.
- 18 ILEGEMS (M.). — Beryllium doping and diffusion in molecular beam epitaxy of GaAs and  $\text{Al}_x\text{Ga}_{1-x}\text{As}$ . *J. Appl. Phys.*, **48**, (1977), 1278-1287.
- 19 CHO (A.Y.), HAYASHI (I.). — P-N junction formation during molecular beam epitaxy of Ge doped GaAs. *J. Appl. Phys.*, **42**, (1971), 4422-4425.
- 20 LANG (D.V.). — Deep level transient spectroscopy. A new method to characterise traps in semiconductors. *J. Appl. Phys.*, **45**, (1974), 3023-3032.
- 21 MILLER (G.L.), LANG (D.V.), KIMERLING (L.C.). — Capacitance transient spectroscopy. *Ann. Rev. Mater. Sci.*, (1977), 337-448.
- 22 LANG (D.V.), CHO (A.Y.), GOSSARD (A.C.), ILEGEMS (M.), WEGMANN (W.). — Study of electron traps in n-GaAs grown by molecular beam epitaxy. *J. Appl. Phys.*, **47**, (1976), 2558-2564.
- 23 BLOOD (P.). — Private communication.